Low-temperature creep of SnPb and SnAgCu solder alloys and reliability prediction in electronic packaging modules

Yuming Zhang,[a,b] Honglai Zhu,[c] Masami Fujiwara,[d] Jinquan Xu[a] and Ming Dao[b,*]

[a]*Department of Engineering Mechanics, Shanghai Jiaotong University, Shanghai 200240, People's Republic of China*
[b]*Department of Materials Science and Engineering, Massachusetts Institute of Technology, Cambridge, MA 02139, USA*
[c]*Beijing Institute of Control Engineering, Haidian District, Beijing 100190, People's Republic of China*
[d]*Division of Applied Physics, College of Engineering, Nihon University, Fukushima 963-8642, Japan*

Creep tests covering a broad temperature range (-40 to $120\,°C$) were systematically performed on Pb5Sn and Sn3Ag0.5Cu solder alloys. Experimental results showed that both solder alloys creep significantly within the temperatures and stress levels tested. A single set of constitutive equations was constructed to describe creep deformation over a wide range of stress and temperature. Numerical analyses revealed that, when evaluating creep failure, significant errors may result from ignoring creep at low temperatures, especially for the lead-free solder alloy Sn3Ag0.5Cu.
© 2012 Acta Materialia Inc. Published by Elsevier Ltd. All rights reserved.

A solder material normally has a relatively low melting temperature, T_m. Creep deformation is the dominant deformation mode in metallic materials when the homologous temperature, $T_H = T/T_m$, exceeds 0.4 [1]. Therefore significant creep can occur at fairly low temperatures [2]. Consequently, creep failure and fatigue failure related to creep are crucial factors in designing reliable electronic packaging modules (EPMs), since their service temperatures are often higher than $0.4T_m$ [3]. Pb5Sn and Sn3Ag0.5Cu solders, for example, with T_m of 456 K (183 °C) and 490 K (217 °C) [2], respectively, may give rise to considerable creep deformation in EPMs even at sub-0 °C temperatures. However, creep studies of solder materials have so far mostly focused on temperatures above room temperature (RT), and only limited reports can be found on the mechanical properties of solders below RT [4,5]. The challenges may be attributed to the difficulties in achieving broad temperature ranges and recording fairly low creep rates (10^{-8}–10^{-10} s^{-1}) [6], along with the (incorrect) impression that most metals and alloys only creep at relatively high temperatures. For example, for circuit boards and/or micro-electromechanical systems (MEMS) devices used in consumer automobiles and aircraft, service temperatures can be much lower than RT or even lower than 0 °C. If there is significant creep deformation at such low temperatures, considerable errors can result when estimating service life if low-temperature creep is not accurately accounted for.

Various forms of creep constitutive equations have been used in the literature to describe different creep mechanisms at different stress levels combined with temperature dependence [2,7–11]. However, none of the individual formulations can be successfully applied to cover all types of solder materials which have to serve a broad range of temperature and stress [12]. Without systematic experimental measurements of low-temperature creep and accurate, experimentally derived constitutive laws for creep, significant errors are expected when attempting to estimate the creep-dominated fatigue life of EPMs due to periodic temperature fluctuations, particularly when the lowest service temperature is lower than 0 °C.

In order to predict creep and fatigue failure of EPMs more reliably, a systematic experimental study was carried out on two types of solders, lead-containing Pb5Sn and lead-free Sn3Ag0.5Cu, at both low- and high-temperature ranges. Pb5Sn is a typical lead-containing solder material that has a simple eutectic microstructure [8]. Sn3Ag0.5Cu is a representative lead-free SnAgCu (SAC) solder material consisting of dispersed

---

* Corresponding author. Tel.: +1 617 253 2100; e-mail: mingdao@mit.edu

precipitates in β-Sn matrix [2], where SAC solders have dominated the lead-free solder market [13]. These two types of solders are expected to exhibit different creep resistances due to their different microstructures. To describe the creep deformation, a single set of phenomenological creep constitutive equations/parameters was extracted based on the experimental results for each solder alloy. The creep laws were then used to estimate the service life of the solder alloys assuming a creep-strain-dominated failure criterion. The results confirmed the importance of accurately accounting for low-temperature creep deformation for both lead-containing and lead-free solders.

The creep behaviors of two types of solder alloys, lead-containing Pb5Sn and lead-free Sn3Ag0.5Cu, with different microstructures [14,15], were tested on an RLD-50 Material Test System (Intelligent Instrument and Equipment Co, Ltd., Changchun, PR China), over the temperature range from 233 to 393 K (−40 to 120 °C). A constant testing temperature was maintained in an insulated environmental chamber which was connected to heating and cooling systems. In high-temperature tests, air was heated by a heating system. In low-temperature tests, liquid nitrogen was absorbed from a pressure tank and pumped into the environmental chamber through two nozzles. The testing system is shown in Figure 1. Bulk samples were used in the experiments. Before creep tests, the specimens were annealed for 24 h at 333 K (60 °C) in vacuum to eliminate residual stress [4]. Accurate strain was obtained directly using a BA120-4AA (ZEMIC, Hanzhong, PR China) strain gage with a valid working temperature range of 273–523 K for the high-temperature tests, and a BA120-5AA (ZEMIC) strain gage optimized for a temperature

in the range of 193–273 K for the low-temperature tests. Constant stress level was applied and maintained during each creep test. Considering temperature dependence and different creep mechanisms under different stress levels, we tested the solder specimens with stress levels ranging from 30% to 90% of their quasistatic yield strengths (strain rate ≈ 0.003 s^{-1}) at each constant temperature.

The results in Figure 2 show that solder alloys creep significantly rather than deform elastically. Regimes I–IV refer to low stress and high temperature, low stress and low temperature, high stress and high temperature, and high stress and low temperature, respectively.

At relatively high stress levels, creep through climb of edge dislocations is usually the dominant deformation mechanism [7], although the details can vary due to differences in microstructure. The distribution of the creep data in Regime IV shows a similar temperature dependence to that in Regime III, indicating that dislocation creep is normally the major deformation mode. Hence, we would expect that creep data in both Regime III and IV can be described by constitutive laws suitable for the dislocation-dominated mechanism.

Coble creep, through grain boundary diffusion, dominates creep deformation at lower stress levels and lower temperatures, while Nabarro–Herring creep, through lattice diffusion, describes well the creep behavior at lower stress levels but relatively high temperatures [7]. The creep data for Sn3Ag0.5Cu in Regime II (low temperature and low stress) displays little temperature dependence, unlike that observed in the other regimes (I, III and IV). In contrast, the creep data for Pb5Sn in Regime II shows a reduced but appreciable temperature dependence compared to that exhibited in the other regimes (I, III and IV). We speculate that the detailed creep mechanisms may be different due to the distinctive microstructures of these two solder alloys [14,15], which give rise to different creep resistances associated with temperature and stress. At low temperature and low stress, Coble creep normally describes diffusion along grain boundaries [7]. If there are hard particles situated on grain boundaries, it can be expected that diffusion along grain boundaries will be impeded by these obstacles. Sn3Ag0.5Cu is such a precipitate-strengthening alloy, and contains high-strength Sn_3Ag and Cu_6Sn_5 particles (Cu_6Sn_5 particles are only present in soldered specimens) [12,14]. Thus, it is likely that the creep resistance of Sn3Ag0.5Cu depends primarily on the amount
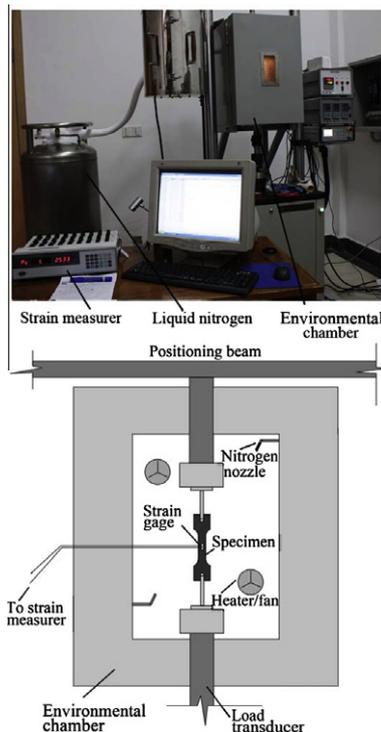
Figure 1. The creep test experimental set-up.
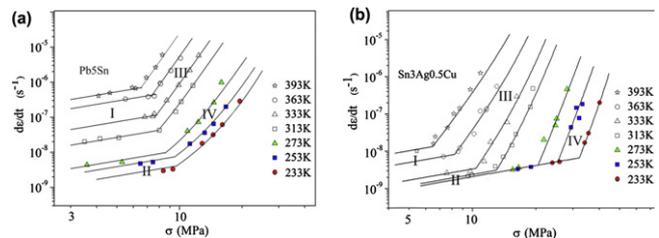
Figure 2. Experimental creep data for (a) Pb5Sn alloy and (b) Sn3Ag0.5Cu alloy. The experimental data points obtained at different testing temperatures are plotted with different symbols. The solid lines are plotted using the constitutive equations, constructed from the entire set of creep data. See text for more details.

of hard precipitates on grain boundaries, with little temperature effect as shown by creep data in Regime II (Fig. 2b).

During Regimes I and II, diffusion creep dominates and the creep mechanisms are characterized by Coble creep and Nabarro–Herring creep. For these creep mechanisms, a linear dependence of creep rate on stress is suitable for describing creep in solder materials [7]. In the regimes with higher stress levels, Regimes III and IV, the linear constitutive relation is no longer suitable when creep rates are much higher due to the activation of dislocation creep mechanisms. The hyperbolic formulation and the power law have been successfully employed to describe creep behavior at different stress levels at higher temperatures [12]. Reviewing various creep constitutive forms as well as the experimental results in Figure 2, which include low-temperature data, none of the available formulations accurately describe the entire data set. In addition, at each temperature T, there exists a critical stress, $\sigma_v(T)$, below which the linear stress-dependent function fits well. Here we propose to solve the dilemma by (i) combining existing formulations with related weighting coefficients, and (ii) adopting a new piecewise formulation separated by the critical linear limit $\sigma_v(T)$. A complete set of functions, which can fit the entire data set encompassing all the tested temperatures and stress levels, is proposed as follows:

$$\dot{\varepsilon} = A_1 \cdot \sigma^{n_1} \cdot \exp\left(-\frac{Q_1}{kT}\right)$$
$$+ A_2 \cdot \sinh^{n_2}(B_2\sigma) \cdot \exp\left(-\frac{Q_2}{kT}\right)$$
$$\text{when } \sigma \geqslant \sigma_v \qquad (1)$$

$$\dot{\varepsilon} = B\sigma \quad \text{when } \sigma < \sigma_v \qquad (2)$$

$$\sigma_v(T) = b_1 \cdot T^3 + b_2 \cdot T^2 + b_3 \cdot T + b_4 \qquad (3)$$

where B is the only temperature-dependent parameter, and k is the Boltzmann constant. The parameters and coefficients in Eq. (1) when $\sigma \geqslant \sigma_v$ can be obtained first by separately fitting the power law (first term) and the hyperbolic formulation (second term), respectively. Then by only varying A_1 and A_2 in Eq. (1), A_1 and A_2 can be determined. To obtain B in Eq. (2), the slopes of the linear fitting curves with stresses below $\sigma_v(T)$ are first summarized. We found that a Boltzmann function and a Boltzmann function corrected by a polynomial term are suitable for fitting Sn3Ag0.5Cu and Pb5Sn data, respectively. Eq. (3) can be subsequently determined by fitting the intersecting points of Eqs. (1) and (2). All parameters and coefficients in the constitutive law are listed in Table 1. These constitutive equations and related parameters are constructed phenomenologically, using a combination of the existing classical creep formulations. We thus expect there would be alternative formulations which could also fit the experimental data well.

With the experimentally determined constitutive laws of Pb5Sn and Sn3Ag0.5Cu alloys accurately describing low-temperature creep, we can now evaluate the errors involved if the low-temperature creep is ignored. To verify the importance of low-temperature creep, two typical cases for each of these two solder alloys were investigated as follows. Two different stress levels, the lower being 7 MPa and the higher 12 MPa, were used to evaluate creep deformation employing Eqs. (1), (2). The accumulated creep strain (ACS), widely accepted as one of the benchmarks for estimating creep and fatigue failure of EPMs [16], can be calculated by imposing thermal cycles on each solder alloy. The repeated temperature variation cycles were set to go up and down between 233 K (−40 °C) and 333 K (60 °C) as shown in Table 2 [17]. With each applied stress level and the assigned thermal cycles, the total creep time (or the total thermal cycles) corresponding to a preset failure ACS strain (5%) for each case can be computed, as shown in Figures 3 and 4. It is clear that Sn3Ag0.5Cu exhibits much longer creep fatigue life than Pb5Sn under the two conditions studied. For comparison, three additional estimations were made by ignoring creep below a set temperature of 253 K (−20 °C), 273 K (0 °C) or 293 K (20 °C), respectively. Figures 3 and 4 show the computed results for Pb5Sn and Sn3Ag0.5Cu, respectively, comparing the baseline case (t_0) which carefully accounted for low-temperature creep with the three cases that ignored low-temperature creep to various degrees.

Table 2. Temperature variation of each cycle during repeated thermal cycling. Temperature is assumed to change linearly during both the heating and cooling periods.

Temperature range	Between −40 and 60 °C
Total time per cycle	4.5 min
Heating period	3 min
Cooling period	1.5 min

Table 1. Parameters and coefficients in Eqs. (1)–(3).

Eq. (1)	A_1 (MPa$^{-n_1}$s^{-1})	n_1	Q_1/k (eV)	A_2 (s^{-1})	B_2 (MPa^{-1})	n_2	Q_2/k (eV)
Pb5Sn	9.66×10^{-6}	8.5	0.63	1.01×10^{-6}	0.182	2.19	0.156
Sn3Ag0.5Cu	9.90×10^{-14}	14.57	0.8	2.01×10^6	0.075	6.85	0.948

Eq. (2)	B(MPa^{-1} s^{-1})
Pb5Sn	$10^{-7} + (7.03 \times 10^{-9} - 10^{-7})/\{1 + \exp[(T - 363.0)/13.87]\} + 8.30 \times 10^{-15}\ T^3 - 6.40 \times 10^{-12}\ T^2$ $+ 1.66 \times 10^{-9}T - 1.5 \times 10^{-7}$
Sn3Ag0.5Cu	$2.43 \times 10^{-9} + (2.05 \times 10^{-10} - 2.43 \times 10^{-9})/\{1 + \exp[(T - 371.1)/13.52]\}$

Eq. (3)	b_1 (MPa K^{-3})	b_2 (MPa K^{-2})	b_3 (MPa K^{-1})	b_4 (MPa)
Pb5Sn	-1.02×10^{-6}	9.98×10^{-4}	-0.34	47.46
Sn3Ag0.5Cu	-3.47×10^{-6}	4.27×10^{-3}	-1.79	262.19

Here t_i, t_{ii} and t_{iii} represent the normalized failure cycles predicted via Eqs. (1)–(3) by ignoring creep below 253 K (−20 °C), 273 K (0 °C) and 293 K (20 °C), respectively.

Obviously, in both Figures 3 and 4, the (over-estimation) error increases with the limiting temperature below which creep deformation is ignored, regardless of the applied stress level. In the worst case (t_{iii} at 7 MPa), ignoring creep below 293 K (20 °C) induces an error as large as 25% for Pb5Sn alloy and 126% for Sn3Ag0.5Cu alloy. The percentage errors are in general much higher for Sn3Ag0.5Cu alloy than for Pb5Sn alloy. As lead-free solder is becoming more widely used, it is clear that an accurate account of low-temperature creep is critical for estimating creep fatigue failure, especially for lead-free alloys.

In summary, this study has extended our knowledge of creep deformation of both lead-containing and lead-free solder alloys into the low-temperature regime. Our investigation revealed that the solder alloys creep significantly at low temperatures rather than only deform elastically. A single set of constitutive equations was constructed to capture creep deformation rates covering a wide range of stress and temperature, including low-temperature regimes. Careful analyses showed that ignoring creep deformation at low temperatures could result in significant errors when estimating creep-strain-dominated fatigue failure. The over-estimation of creep fatigue life was found to be much higher for the lead-free Sn3Ag0.5Cu alloy than for the lead-containing Pb5Sn alloy. The findings in the present study provide systematic and quantitative experimental data sets, suggest a practical way to construct the creep constitutive law covering wide ranges of stress and temperature, and offer new insights into the low-temperature creep of both lead-containing and lead-free solder alloys. The newly obtained understanding will be of great importance for designing circuit boards and/or MEMS devices intended for low-temperature service conditions.

Figure 3. Normalized creep failure time (cycles) for Pb5Sn solder alloy, t_0, as compared to the three cases, t_i, t_{ii} and t_{iii}, obtained by ignoring creep deformation below 253 K (−20 °C), 273 K (0 °C) and 293 K (20 °C), respectively. The applied loads are set to be (a) 7 MPa and (b) 12 MPa, and the thermal cycles are defined in Table 2. A preset creep failure strain is taken to be 5%.
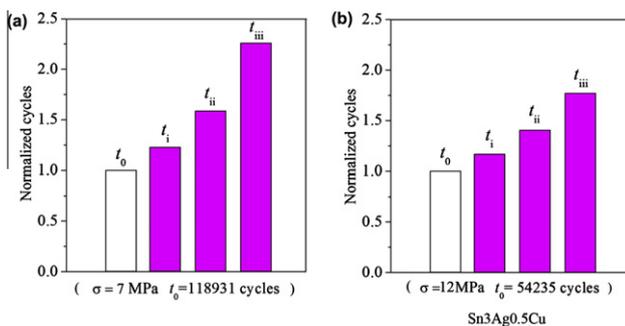
Figure 4. Normalized creep failure time (cycles) for Sn3Ag0.5Cu solder alloy, t_0, as compared to the three cases, t_i, t_{ii} and t_{iii}, obtained by ignoring creep deformation below 253 K (−20 °C), 273 K (0 °C) and 293 K (20 °C), respectively. The applied loads are set to be (a) 7 MPa and (b) 12 MPa, and the thermal cycles are defined in Table 2. A preset creep failure strain is taken to be 5%.

[1] J. Cadek, Creep in Metallic Materials, Elsevier, Amsterdam, 1988.
[2] H. Ma, J.C. Suhling, J. Mater. Sci. 44 (2009) 1141–1158.
[3] C. Kanchanomai, Y. Mutoh, Scripta Mater. 50 (2004) 83–88.
[4] J.H.L. Pang, B. Xiong, T. Low, in: Proc. 54th Electronic Components and Technology Conference, IEEE, 2004, pp. 1333–1337.
[5] X. Shi, Z. Wang, W. Zhou, H. Pang, Q. Yang, J. Electron. Packaging 124 (2002) 85–90.
[6] M. McLean, Acta Metall. 33 (1985) 545–556.
[7] T. Courtney, Mechanical Behavior of Materials, McGraw-Hill, New York, 1990.
[8] S. Wiese, F. Feustel, E. Meusel, Sens. Actuators A Phys. 99 (2002) 188–193.
[9] A. Schubert, R. Dudek, E. Auerswald, A. Gollbardt, B. Michel, H. Reichl, in: Proc. 53rd, Electronic Components and Technology Conference, IEEE, 2003, pp. 603–610.
[10] H. Takagi, M. Dao, M. Fujiwara, M. Otsuka, Philos. Mag. 83 (2003) 3959–3976.
[11] H. Takagi, M. Dao, M. Fujiwara, M. Otsuka, Mater. Trans. JIM 47 (2006) 2006–2014.
[12] S. Wiese, K.J. Wolter, Microelectron. Reliab. 44 (2004) 1923–1931.
[13] Soldertec European Lead-free Roadmap, 2002;1:1–26
[14] J. Zhao, Y. Miyashita, Y. Mutoh, Int. J. Fatigue 22 (2000) 665–673.
[15] K.S. Kim, S.H. Huh, K. Suganuma, Microelectron. Reliab. 43 (2003) 259–267.
[16] A. Syed, in: Proc. 54th Electronic Components and Technology Conference, IEEE, 2004, pp. 737–746.
[17] I. Kim, S.-B. Lee, in: Proc. 57th, Electronic Components and Technology Conference, IEEE, 2007, pp. 95–104.